https://doi.org/10.48048/tis.2023.5529

Plant-derived Antiviral Compounds as Potential COVID-19 Drug Candidates: *In-silico* Investigation in Search of SARS-CoV-2 Inhibitors

Bhaskor Kolita[1,*], Dimplly Borah[1], Pinaki Hazarika[1], Ely Phukan[2] and Rashmi Rekha Borah[1]

[1]*Department of Botany, Jorhat Kendriya Mahavidyalaya, Jorhat 785010, Assam, India*
[2]*Department of Zoology, Jorhat Kendriya Mahavidyalaya, Jorhat 785010, Assam, India*

([*]Corresponding author's e-mail:bhaskorkalitabioinfo@gmail.com)

Received: 7 August 2022, Revised: 11 September 2022, Accepted: 18 September 2022, Published: 31 May 2023

Abstract

Corona virus disease 2019 (COVID-19) is an infectious disease caused by SARS-CoV-2, a newly discovered pathogenic corona virus that causes respiratory illness in humans and has now become a major challenge for the entire world. Although several vaccines for COVID-19 have been approved to date, lead compounds are still in high demand for the development of more promising or effective drugs and vaccines. According to the literature, antiviral drugs are used to treat COVID-19; thus, the current study is an attempt to screen lead molecules from plant-derived antiviral compounds. In this study, 33 plant-derived compounds with antiviral properties against corona viruses were used as ligand molecules, with Favilavir, Remdesivir, Ivermectin, and Dexamethasone serving as reference drugs. Molecular docking was performed between the selected ligands and the four main drug targets of SARS-CoV-2, Nucleocapsid Protein, Spike Glycoprotein, Proteases 3CLpro, and Helicase, and ADMET properties of screened compounds were observed. Docking results revealed that Reserpine, Tetrandrine, and Xanthoangelol F had a high Moldock score with each target, just like the current COVID-19 medications, Ivermectin and Remdesivir. Docking and ADMET studies indicate that Reserpine, Tetrandrine, and Xanthoangelol F may be potent lead compounds for the treatment of COVID-19 and should be investigated further.

Keywords: COVID-19, SARS-CoV-2, Antiviral, Molecular docking, ADMET

Introduction

COVID-19 is caused by Severe Acute Respiratory Syndrome corona virus 2 (SARS-CoV-2), a newly discovered highly pathogenic human corona virus (CoV). This was first reported in Wuhan, China, in December 2019 and quickly became a global pandemic [1,2].

According to the WHO COVID-19 Weekly Epidemiological Update- 19 - 31 August 2022, over 598 million confirmed cases and over 6.4 million deaths have been reported globally [3]. COVID-19 has become the greatest threat to humanity due to its epidemic nature and a lack of appropriate and effective drugs.

SARS-CoV-2, like SARS-CoV and the Middle East respiratory disease corona virus (MERSCoV), is a member of the Coronaviridae family. These three viruses are zoonotic, meaning they can cause serious infection in humans, as opposed to other human CoVs (HCoV-NL63, HCoV-229E, CoV-OC43, and HCoVHKU1), which are only responsible for minor respiratory infections [4]. The genomic sequence of SARS-CoV-2 revealed that it shares 82 percent sequence identity with SARS-CoV and, to a lesser extent, MERSCoV [5,6]. The pharmacological target of SARS-CoV-2 can be recognized from the life cycle of CoVs due to sequence similarity [7].

In the search for SARS-CoV-2 therapeutic options, all CoV enzymes and proteins involved in viral replication and control of host cellular machinery are potentially druggable targets. The Nucleocapsid Protein of Corona virus is an interesting therapeutic target since it plays a vital function in viral RNA transcription and replication [8]. Kang *et al.*[9] crystallized the SARS-CoV-2 nucleocapsid N-terminal domain, which has been structured and relocated in the Protein Data Bank (PDB ID: 6M3M) and is publicly available. Spike (S) Glycoprotein in CoVs mediates virus entry by contacting specific host-receptors on the cell's surface and is an intriguing pharmacological target [10]. Wrapp et al. crystallized SARS-CoV-2 spike glycoprotein and repositioned it in the Protein Data Bank (PDB ID: 6VSB) [11].

Proteases 3CLpro (3C-like protease or main protease) are crucial for virus replication and controlling the host cell response; therefore, they stand as key targets in the development of antiviral drugs [12,13]. Liu *et al.* [14] determined the crystal structure of COVID-19 main protease protein from COVID-19(PDB code: 6LU7). Helicase in CoVs catalyzes the separation of duplex oligonucleotides into single strands in a nucleotide triphosphate (NTP) hydrolysis-dependent manner. This protein is essential for RNA viral synthesis and considered an interesting target for drug development [15]. At the time of this *in-silico*study, no structural information on the SARS-CoV-2 helicase was available, but structural information on SARS-CoV was available (PDB code: 6JYT) [16]. The availability of the SARS-CoV structure, which has a high sequence similarity (99.8 percent), significantly encourages the search for drugs to treat COVID-19.

Even though many drugs have been tried for COVID-19, none have been approved. As a result, drug repurposing has emerged as a new hope for combating the COVID-19 pandemic. Drug repositioning is a strategy for accelerating drug discovery by repurposing existing pharmaceuticals for diseases other than their primary indications [17]. Following the emergence of the COVID-19 pandemic, several drug candidates from the existing drug repository were assessed for activity against SARS-CoV-2. Identification of drugs with high target specificity, as well as the discovery of existing drugs that could be repurposed to treat SARS-CoV-2 infection, is critical for this purpose [18]. Favilavir, an anti-viral drug, has been shown to be effective in treating the symptoms of COVID-19 in a clinical trial of more than 70 patients with minimal side effects [19]. Remdesivir demonstrated efficacy in animals by resisting two viruses like Covid-19, SARS-CoV and MERS-CoV. One 35-year-old man recovered from COVID-19 in a clinical trial of Remdesivir [20,21]. Remdesivir, a SARS-CoV-2 treatment approved by the FDA for emergency use, targets the RNA-dependent RNA polymerase (RdRp) enzyme of SARS-CoV-2 [22]. In an *in-vitro* study conducted in Australia [23], an anti-parasitic drug known as ivermectin was shown to be effective against the SARS-CoV-2 virus. Dexamethasone, a corticosteroid, can save the lives of COVID-19 patients who are critically ill [24]. These current medications of COVID-19 were taken in this *in-silico* study as reference.

Plant-derived compounds are known to be a rich source of lead compounds for drug discovery. A review conducted by Ebob *et al*. [25] suggested that compounds from the alkaloid, flavonoid, terpenoid, phenolic, xanthone, and saponin classes could be lead compounds against SARS-COV-2, as they demonstrated activities at less than 10 μM against the coronaviruses. Several natural products have demonstrated potent antiviral activity against SARS-CoV [26-28], MERS-CoV [29], HCoV-229E [30], and HCoV-OC43 [31]. The study of these natural compounds *in-silico*, *in-vitro*, and *in vivo* will aid in the discovery of a drug for SARS-COV-2.Taking these perspectives into account, we chose Favilavir, Remdesivir, Ivermectin, Dexamethasone, and 33 plant-derived antiviral compounds with good IC_{50} values against CoVs for our study of SARS-CoV-2 inhibitors.

Materials and methods

Compound selection

We chose 33 plant-derived compounds with antiviral activity against CoVs as ligands from various research articles [32-43]. As reference drugs, we chose the antiviral drugs Favilavir and Remdesivir, as well as the antiparasitic drug Ivermectin and the steroid Dexamethasone. The selected antiviral compounds with IC_{50} against CoVs are in **Table 1**.

Table 1 Plant-derived antiviral compounds with IC_{50} value against SARS-CoV and references.

Compound	IC_{50}	Compound	IC_{50}	Compound	IC_{50}
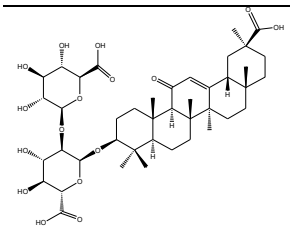 Glycyrrhizin	300 mg/L (SARS-CoV) [32]	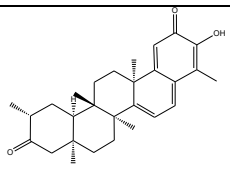 Tingenone	9.9 µmol/L (SARS-CoV)[38]	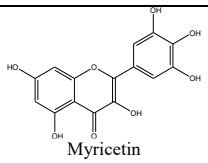 Myricetin	2.71±0.19 µmol/L (SARS-CoV)[42]
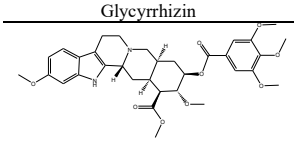 Reserpine	6.0 µmol/L (SARS-CoV)[26]	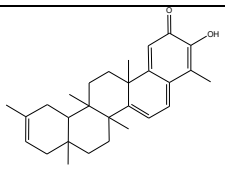 Iguesterin	2.6 µmol/L (SARS-CoV)[26]	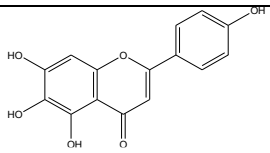 Scutellarein	0.86±0.48 µmol/L (SARS-CoV)[42]
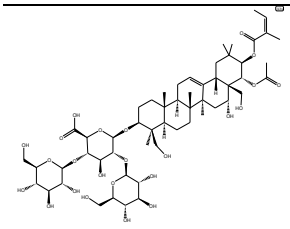 Aescin	3.4 µmol/L (SARS-CoV)[26]	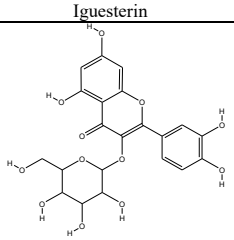 Quercetin-3-β-galactoside	42.79±4.97 µmol/L (SARS-CoV)[39]	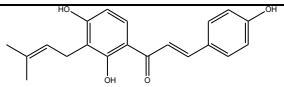 Isobavachalcone	39.4 ± 5.2 µmol/L (SARS-CoV)[43]
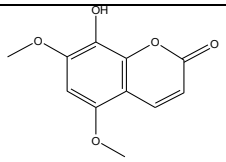 Leptodactylone	100 µg/mL (SARS-CoV)[33]	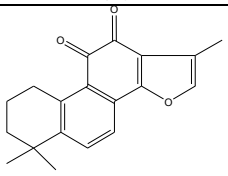 Tanshinone I	1.6 ± 0.5b µmol/L (SARS-CoV)[40]	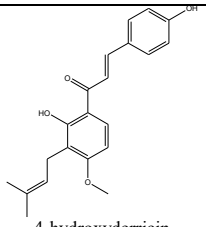 4-hydroxyderricin	81.4 ± 8.5 µmol/L (SARS-CoV)[41]
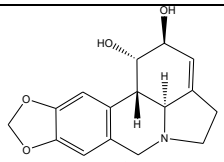 Lycorine	15.7 ± 1.2 nmol/L (SARS-CoV)[34]	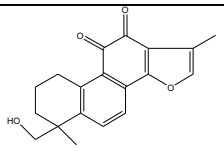 Tanshinone II	10.7 ± 1.7 µmol/L (SARS-CoV)[40]	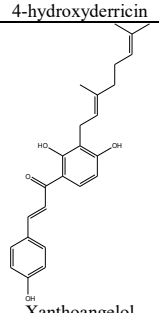 Xanthoangelol	38.4 ± 3.9 µmol/L (SARS-CoV)[43]
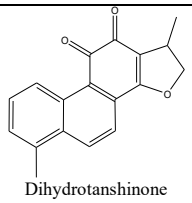 Dihydrotanshinone	1 µg/Ml (MERS-CoV)[35]	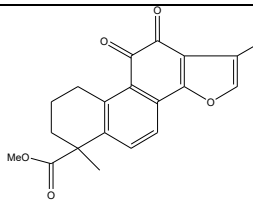 Tanshinone III	9.2 ± 2.8 µmol/L (SARS-CoV)[40]	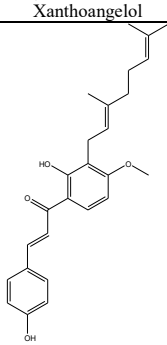 Xanthoangelol F	34.1 ± 4.8 µmol/L (SARS-CoV)[43]

Compound	IC_{50}	Compound	IC_{50}	Compound	IC_{50}
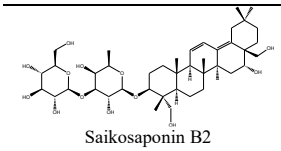 Saikosaponin B2	1.7±0.1 µmol/L (HCoV-229E) [34]	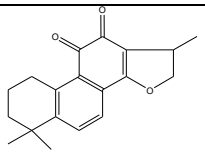 Tanshinone IV	0.8 ± 0.2 µmol/L(SARS-CoV)[40]	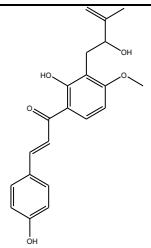 Xanthoangelol D	26.6 ± 5.2 µmol/L (SARS-CoV)[43]
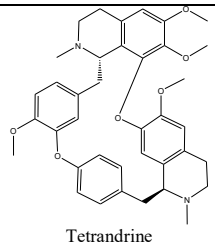 Tetrandrine	0.33±0.03µmol/ L (HCoV-OC43)[36]	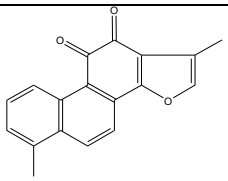 Tanshinone V	8.8 ± 0.4 µmol/L (SARS-CoV)[40]	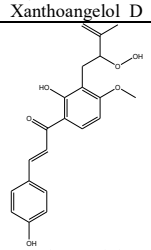 xanthoangelol E	11.4 ± 1.4 µmol/L (SARS-CoV)[43]
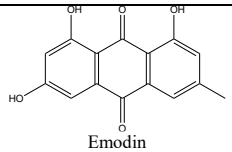 Emodin	200 µmol/L (SARS-CoV)[37]	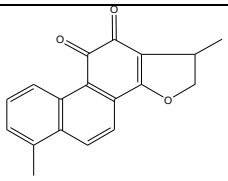 Tanshinone VI	4.9 ± 1.2 µmol/L (SARS-CoV)[40]	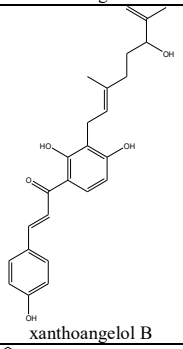 xanthoangelol B	22.2 ± 6.5 µmol/L (SARS-CoV)[43]
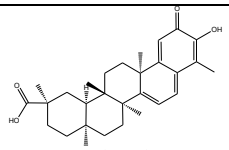 Celastrol	10.3 µmol/L (SARS-CoV)[38]	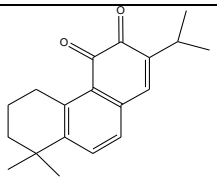 Tanshinone VII	30.0 ± 5.5 µmol/L(SARS-CoV)[40]	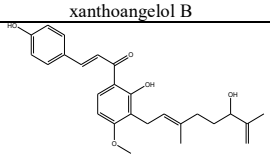 xanthoangelol G	129.8 ± 10.3 µmol/L (SARS-CoV)[43]
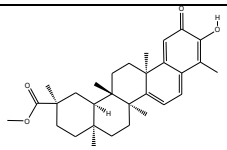 Pristimererin	5.5 µmol/L (SARS-CoV)[38]	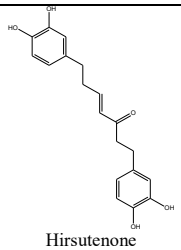 Hirsutenone	4.1µmol/L (SARS-CoV)[40,41]	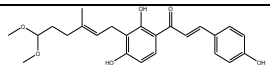 xanthokeistal A	44.1 ± 1.3 µmol/L (SARS-CoV)[43]

Molecular docking

The crystal structures of CoV-2 nucleocapsid N-terminal domain (6M3M), COVID-19 main protease (6LU7), nucleocapsid N-terminal domain(6M3M), and helicase of SARS-CoV (6JYT) were downloaded from PDB. ChemDraw Ultra 12.0.2.1076 (Cambridge Soft, UK) was used for ligand preparation. 2D structures of the ligands were drawn and then converted into 3D. ChemDraw 3D was used for 3D chemical structure optimization and energy minimization of the selected compounds and reference drug compounds, with 0.1 RMS gradient for geometry optimization. The protein preparation tab of Molegro Virtual Docker (MVD) was evoked for removing attached ligand, water and co-factors. Hybridization state, bond order and explicit hydrogen were assigned in the automatic preparation mode and charges were assigned according to the scoring function used (MolDock Scoring Function).

Grid-based cavity prediction algorithm of MVD was used for predicting the binding sites of the protein where grid resolution was kept at 0.8 Å covering the protein. Accessibility of the grid points was checked with the placement of spheres of radius 1.4 Å determined by the Van der Waals for overlap analysis and random directions were chosen from the accessible grid point to survey if any inaccessible grid point hits on the way which was repeated for 16 different directions giving its accessibility if 12 or more of these lines hit an inaccessible volume. Volumes below 10.0 Å3 were discarded as irrelevant after connecting the neighboring grid points [44]. Predicted active site cavities were scored and ranked according to their volumes and the highest-scoring ones were selected for each protein. The properties of the selected cavities of each target can be seen in (**Table S1 of supplementary material**).

Selected ligands and four current COVID-19 medications were allowed to dock with the residues of each protein's detected cavity separately using MolDock Score (GRID) as the docking algorithm in Molegro virtual docker (MVD) and energy potential evaluation were done for the grid points based on tri-linear interpolation. The scoring function MolDock SE (Simplex Evolution) was used, with a maximum iteration of 1500 for a population size of 50 and 5 runs. Poses were generated from the initial population size, and different torsion angles (sp2-sp2, sp2-sp3, or sp3-sp3), translation, and rotation were considered for evaluating the most affected part of the molecule and rewarding the lowest conformation. For pose generation, the energy threshold was set to 100, and the poses were clustered using the Tabu clustering technique of MVD with an RMSD threshold of 2.00, taking into account the intrinsic ligand symmetries. Following docking, the best poses were chosen for further analysis based on docking scores (MolDock Score), which is a statistical scoring function that converts interacting energy into numerical values [45,46]. The top 10 repeated poses in each target were then converted to the ligand, and H-bond interactions between the ligand and the selected targets were investigated.

ADME and toxicity prediction

In admetSAR1, the ADME properties and toxicity characteristics of three best results ligands and two reference drugs were investigated. In admetSAR1, 27 quantitative structure-activity relationships (QSAR) models are compiled from the scientific literature for ADMET prediction, including 22 qualitative classification and 5 quantitative regression models of over 2 lakhs ADMET annotated data points for over 96 thousand unique compounds [47].

Results and discussion

Molecular docking

In this study, we used 37 compounds as ligands, including the antiviral drugs Favilavir and Remdesivir, as well as the anti-parasitic drug Ivermectin, the steroid Dexamethasone, and 33 plant-derived antiviral compounds with high IC50. MVD was used to perform molecular docking between the selected ligands and SARS-CoV-2 target proteins.

The antiviral potential of selected ligands was assessed by analyzing their post docking interactions and scores with four SARS-CoV-2 pharmacological targets. The MolDock Score (kcal/mol) was used to evaluate the docking results. The docking results for the selected ligands and four targets are shown in Table S2of supplementarymaterial. For each target, we chose the top ten ligands based on MolDock Score for further investigation in **Table 2**.

Table 2 Top 10 docking result in 4 selected targets.

Spike Glycoprotein (6VSB)		Nucleocapsid N-terminal domain (6M3M)		COVID-19 main protease protein (6LU7)		Helicase (6JYT)	
Ligand	**MolDock Score (kcal/mol)**	**Ligand**	**MolDock Score (kcal/mol)**	**Ligand**	**MolDock Score (kcal/mol)**	**Ligand**	**MolDock Score (kcal/mol)**
*Ivermectin	−146.91	*Ivermectin	−159.38	*Remdesivir	−162.52	*Ivermectin	−183.22
*Remdesivir	−127.12	*Remdesivir	−153.99	Quercetin-3-b-galactoside	−162.24	Reserpine	−147.82
Reserpine	−115.02	Aescin.MOL	−153.16	Reserpine	−162.22	*Remdesivir	−140.83
Xanthoangelol F	−110.86	Glycyrrhizin	−139.98	*Ivermectin	−159.15	Glycyrrhizin	−139.65
Aescin	−107.61	Reserpine	−139.45	Xanthoangelol F	−158.30	Aescin	−139.44
Tetrandrine	−106.95	Xanthoangelol	−137.81	Tetrandrine	−156.93	Tetrandrine	−137.68
Xanthoangelol	−106.04	Tetrandrine	−133.52	Xanthoangelol	−151.89	xanthoangelol G	−130.40
Xanthoangelol G	−105.20	Xanthoangelol G	−125.77	Xanthoangelol B	−147.84	Xanthokeistal A	−130.35
Xanthoangelol B	−99.10	Xanthoangelol F	−122.77	Xanthoangelol D	−147.16	Xanthoangelol B	−128.03
Isobavachalcon	−98.56	4-hydroxyderricin	−121.17	Xanthokeistal A	−144.28	Xanthoangelol F	−128.03

*Drug compound

We observed that three antiviral compounds, namely Reserpine (IC50 value 6.0 mol/L against SARS-CoV) 26, Tetrandrine (IC50 value 0.330.03 mol/L against HCoV-OC43) 36, and Xanthoangelol F (IC50 value 34.1 4.8 mol/L against SARS-CoV) 43, had good docking scores with each of the 4 selected target proteins of SARS-CoV-2 in **Table 2**. The H-Bond interaction between the best ligand and each of the selected target proteins was then investigated.

H-Bond interaction

H-Bond interactions are weak and easily broken, but they play a key role in protein-ligand interactions as well as in ligand-protein interaction stabilization [48,49]. In this context, the best-performing ligands in each protein were chosen to observe H-Bond interactions concerning to the residues involved (**Figures 1 - 3** and **S1 - S2 of supplementary material**).

Reserpine, Tetrandrine, and Xanthoangelol F, as well as the drugs Remdesivir and Ivermectin, demonstrated good H-bonding with each protein. Remdesivir, an antiviral drug, had the best H-bond interaction with each target, followed by Xanthoangelol F, Ivermectin, Reserpine, and Tetrandrine in **Table 3**.

Table 3 Hydrogen bonding pattern at the binding sites of the targets.

Compound	H-bond with Spike Glycoprotein (6VSB)	H-bond with COVID-19 main protease (6LU7)	H-bond with Nucleocapsid N-terminal domain (6M3M)	H-bond with Helicase (6JYT)
*Ivermectin	O (Tyr 313)-H-O O (Lys 310)-H-O N (Arg 1014)-H-O	O (Thr 24)-H-O O (Thr 25)-H-O S (Cys 145_-H-O O (Glu 166)-H-O O (Gln 192)-H-O	N (Arg 150)-H-O O (Tyr 124)-H-O O (Trp 133)-H-O N (Lys 66)-H-O	O (Thr 199)-H-O P (Phe 200)-H-O N(Arg 178)-H-O N(Ala 379)-H-O O(Pro 406)-H-O
Reserpine	O (Leu 303)-H-O O (Gln 957)-H-O N (Gln 957)-H-O N (Gln 314)-H-O	N (His 163-H-O S (Cys 145)-H-O N (Gly 143)-H-O O (Ser 46)-H-O	O (Tyr 112)-H-O O (Phe 67)-H-O O (Trp 133)-H-O	O (Thr 410)-H-O N (His 311)-H-O N (Arg 339)-H-O N (Arg 178)-H-O
*Remdesivir	N(Asn 960)-H-O O(Gln 957)-H-O O(Asp 950)-H-O	O (Thr 26)-H-O N (Thr 26)-H-O O (Gln 189)-H-O O (His 164)-H-O O (His 41)-H-N N (Gly 143)-H-O	O(Thr 149)-H-N O(Lys 128)-H-N N (Lys 128)-H-O O(Ala 126)-H-O N(Trp 133)-H-O O(lle 131)-H-O	O(Leu 176)-H-O O(Thr 410)-H-N N(Arg 409)-H-N N(Asn 179)-H-N N(Asn 177)-H-O O(Asp 534)-H-O N(Asn 519)-H-O
Tetrandrine	N(Leu 945)-H-O	O(Ser 144)-H-O	Nil	N(Arg 178)-H-O N (Arg 339-H-O O(Ser 310)-H-O N(His 311)-H-O
Xanthoangelol F	O(Asp 950)-H-O N(Asn 953)-H-O N(lle 312)-H-O O(lle 312)-H-O	S(Cys 145)-H-O O (Asn 142)-H-O N (Gln 192)-H-O N (Thr 190)-H-O O (Ser 144)-H-O	O(Thr 167-H-O N(Lys 66)-H-O O(Glu 63)-H-O	O(Gln 537)-H-O O(Asp 534)-H-O N(Ala 379)-H-O

*Drug compound

Binding mode of Reserpine

Reserpine had an interacting energy of −115.02 kcal/mol with Spike Glycoprotein, −139.45 kcal/mol with Nucleocapsid N-terminal domain, −162.22 kcal/mol with COVID-19 main protease protein, and -147.82 kcal/mol with Helicase. It also showed inhibition potential by showing four H-Bond interacting with Leu 303, Gln 957, Gln 314 of Spike Glycoprotein, four H-Bond interacting with His 163, Cys 145, Gly 143, Ser 46 of COVID-19 main protease protein, three H-Bond interacting with Tyr 112, Phe 67, Trp 133 of Nucleocapsid N-terminal domain and four H-Bond interacting with Thr 410, His 311, Arg 339, Arg 178 of Helicase in **Figure 1**.

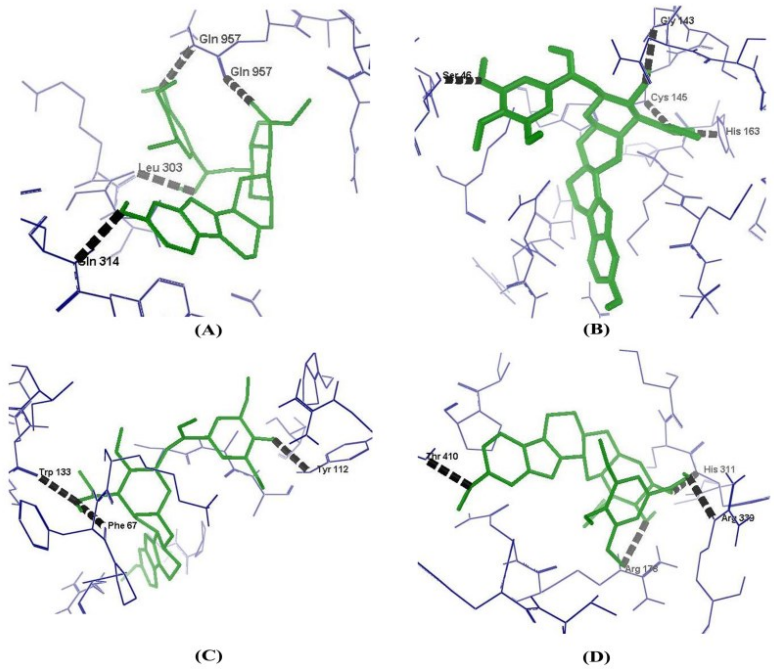

Figure 1 Residues interacting with Reserpine forming Hydrogen bonds (black dash lines) in (a) spike glycoprotein of SARS-CoV-; (b) COVID-19 main protease protein; c) SARS-CoV-2 nucleocapsid N-terminal domain;(d) helicase of CoV.

Binding mode of Tetrandrine

Tetrandrine had an interacting energy of −106.95 kcal/mol with Spike Glycoprotein, −133.52 kcal/mol with Nucleocapsid N-terminal domain, −156.93 kcal/mol with COVID-19 main protease protein, and -137.68 kcal/mol with Helicase. **Figure 2** also showed inhibition potential by displaying one H-Bond interacting with Spike Glycoprotein Leu 945, 1 H-Bond interacting with COVID-19 main protease protein Ser 144, and four H-Bond interacting with Helicase Arg 178, Arg 339, Ser 310, and His 311 but no H-Bond interacting with Nucleocapsid N-terminal domain.

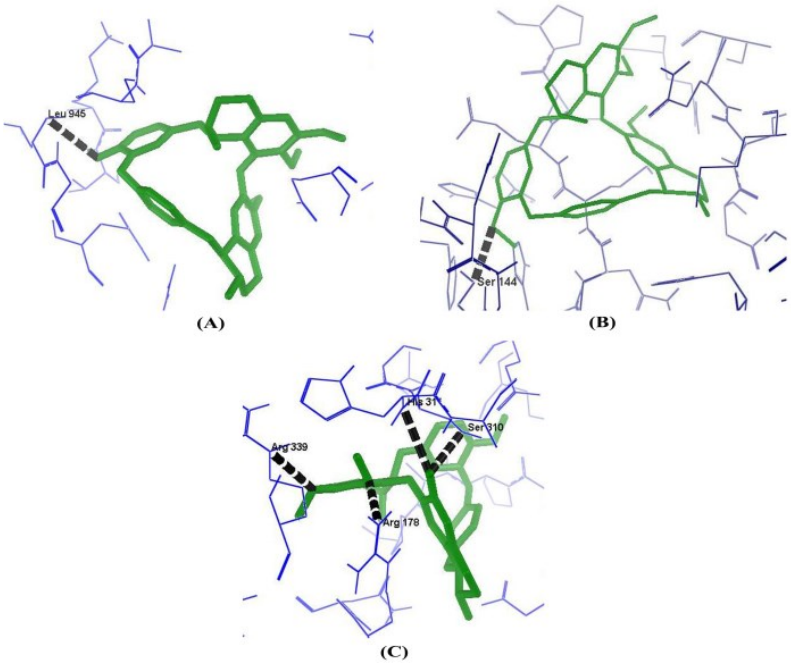

Figure 2 Residues interacting with Tetrandrine forming Hydrogen bonds (black dash lines) in (a) spike glycoprotein of SARS-CoV-; (b) COVID-19 main protease protein; c) helicase of CoV.

Binding mode of Xanthoangelol F

XanthoangelolF had an interacting energy of −110.86 kcal/mol with Spike Glycoprotein, −122.77 kcal/mol with Nucleocapsid N-terminal domain, −158.30 kcal/mol with COVID-19 main protease protein, and −128.03 kcal/mol with Helicase. It also showed inhibition potential by showing four H-Bond interacting with Asp 950, Asn 953, lle 312 of Spike Glycoprotein, 5 H-Bond interacting with Cys 145, Asn 142, Gln 192, Thr 190, Ser 144 of COVID-19 main protease protein, three H-Bond interacting with Thr 167, Lys 66, Glu 63 of Nucleocapsid N-terminal domain and three H-Bond interacting with Gln 537, Asp 534, Ala 379 of Helicase in **Figure 3**.

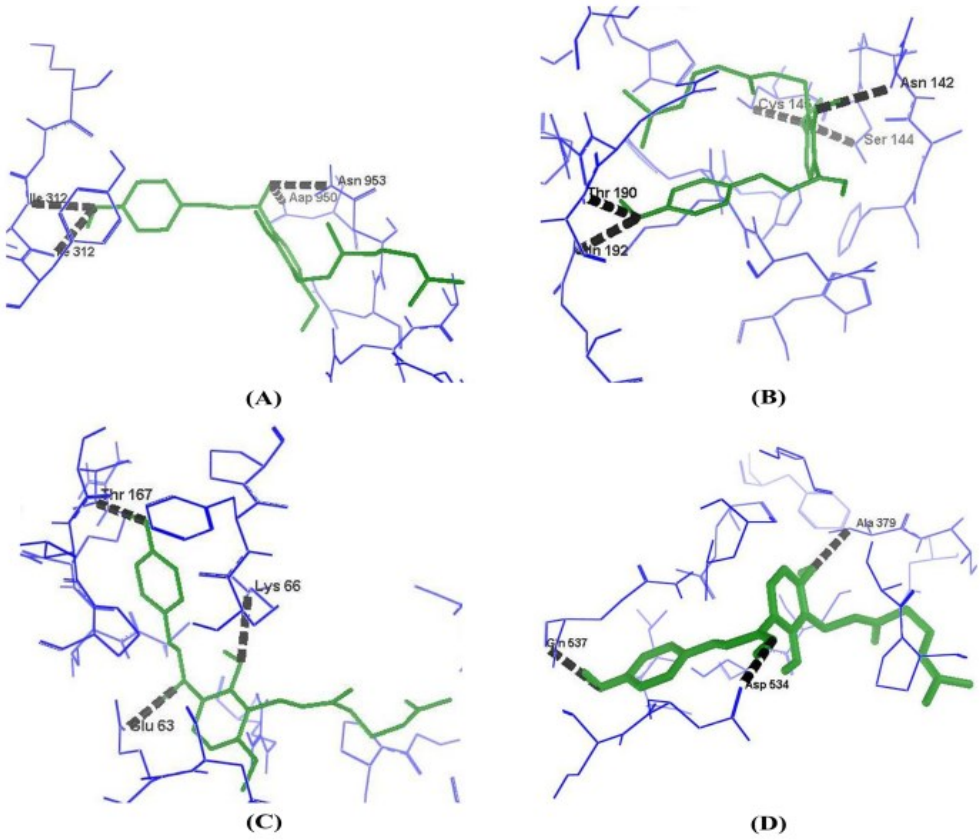

Figure 3 Residues interacting with Xanthoangelol F forming Hydrogen bonds (black dash lines) in (a) spike glycoprotein of SARS-CoV-; (b) COVID-19 main protease protein; (c) SARS-CoV-2 nucleocapsid N-terminal domain;(d) helicase of CoV.

We discovered that the ligands Reserpine, Tetrandrine, and Xanthoangelol F had good docking results and H-bond interation with different essential proteins of SARS-CoV-2, such as Nucleocapsid Protein, Spike Glycoprotein, Proteases 3CLpro, and Helicase, which play critical roles in viral RNA transcription and replication [8]. Because the compound has a high interacting energy and has formed H-Bonds with the essential proteins of SARS-CoV-2, it may be able to suppress SARS-CoV-2 replication.

ADME and toxicity study

Absorption, distribution, metabolism, excretion, and toxicity (ADMET) properties play key roles in the discovery or development of drug candidates. We predicted various ADMET properties in admetSAR1, including Blood-Brain Barrier (BBB) penetration, Human Intestinal Absorption (HIA), Caco-2 Permeability (Caco-2) CYP metabolism, AMES toxicity, and Carcinogens in **Table 4**.

Table 4 ADMET properties of the best results compounds.

Compound	Absorption			Metabolism						Toxicity	
	Blood-Brain Barrier	Human Intestinal Absorption	Caco-2 Permeability	CYP450 2C9 Substrate	CYP450 2D6 Substrate	CYP450 3A4 Substrate	CYP450 1A2 Inhibitor	CYP450 2C19 Inhibitor	CYP450 2D6 Inhibitor	AMES Toxicity	Carcinogens
*Ivermectin	BBB+	HIA+	CaCO2-	[a]n.s	[a]n.s	[b]s	[d]n.i	[d]n.i	[d]n.i	Non AMES	Non Carcinogenes
Reserpine	BBB+	HIA+	CaCO2+	[a]n.s	[a]n.s	[b]s	[d]n.i	[d]n.i	[d]n.i	Non AMES	Non Carcinogens
*Remdesivir	BBB-	HIA-	CaCO2-	[a]n.s	[a]n.s	[b]s	[d]n.i	[d]n.i	[d]n.i	Non AMES	Non Carcinogens
Tetrandrine	BBB+	HIA+	CaCO2+	[a]n.s	[b]s	[b]s	[d]n.i	[d]n.i	[d]n.i	AMES toxic	Non Carcinogens
Xanthoangelol F	BBB+	HIA+	CaCO2+	[a]n.s	[a]n.s	[b]s	[c]i	[c]i	[d]n.i	Non AMES	Non Carcinogens

[a]n.s. = non substrate, [b]s= substrate, [c]i= inhibitor, [d]n.i.=non inhibitor
*Drug compound

We observed that the three plant-derived antiviral compounds with a high MolDock score in each target showed positive Blood-Brain Barrier (BBB) penetration, Human Intestinal Absorption (HIA), and Caco-2 Permeability (Caco-2) while the antiviral drug Remdesivir showed negative, indicating that these compounds are more active than the drug. Human cytochrome P450s (CYPs), a superfamily of heme-containing enzymes with approximately 57 isoforms, catalyze the metabolism of a diverse range of endogenous and xenobiotic compounds [50]. Among the various types of metabolic reactions, oxidative reactions are the most important and prevalent; all drugs for phase I biotransformation undergo oxidation at some point, and CYP enzymes, specifically IA2, 2C9, 2C19, 2D6 and 3A4 are responsible for approximately 90 % of oxidative metabolic reactions [51].

In the last several decades, several commercial drugs were withdrawn from the market due to adverse CYP enzyme drug interactions [52,53]. In our study, we used admetSAR1 to predict the possible metabolic pathways of the screened compounds, and we observed that all of them were CYP450 3A4 substrates (Table 4). We observed that the selected ligands were noncarcinogenic in the toxicity study performed in admetSAR. However, lead Tetrandrine exhibited AMES Toxicity (**Table 4**).

Conclusions

This *in-silico* study revealed that plant-derived antiviral compounds are effective inhibitors of multiple targets, including Nucleocapsid Protein, Spike Glycoprotein, Proteases 3CLpro, and SARS-CoV-2 Helicase.

In terms of docking scores and H-Bond interaction, three ligands, Reserpine, Tetrandrine, and Xanthoangelol F, outperformed the reference drug Remdesivir. The interaction energy and H-Bond interaction profile indicated that they had the potential to inhibit SARS-CoV-2 replication.

Various pharmacokinetic parameters such as oral absorption, plasma protein binding, possible metabolic pathway by different CYP enzymes, and possible CYP inhibition, as well as toxicity characteristics such as carcinogenicity and AMES Toxicity, were evaluated, indicating that the three compounds are pharmacologically active. As a result, Reserpine, Tetrandrine, and Xanthoangelol F have a high potential for use in the treatment of SARS-CoV-2. It should be noted that the study's limitation is related to the reality of *in-silico* studies. It could be concluded that it requires verification through *in-vitro* and *in-vivo* studies, as well as clinical trials, which could support our investigations.

Acknowledgements

We gratefully acknowledge the support of the principal and all faculty members of the science stream at Jorhat Kendriya Mahavidyalaya, Kenduguri, Jorhat, Assam, India.

References

[1] X Xu, P Chen, J Wang, J Feng, H Zhou, X Li, W Zhong and P Hao. Evolution of the novel Corona virus from the ongoing Wuhan outbreak and modeling of its spike protfein for risk of human transmission. *Sci. Chin. Life Sci.* 2020; **63**, 457-60.

[2] I Chakraborty and P Maity. COVID-19 outbreak: Migration, effects on society, global environment, and prevention. *Sci. Total Environ.* 2020; **728**, 138882.

[3] Weekly epidemiological update on COVID-19, Available at: https://www.who.int/publications/m/item/weekly-epidemiological-update-on-covid-19---31-august-2022, accessed August 2022.

[4] J Cui, F Li and ZL Shi. Origin and evolution of pathogenic Corona viruses. *Nat. Rev. Microbiol*. 2019; **17**, 181-92.

[5] F Wu, S Zhao, B Yu,YM Chen, W Wang, ZG Song, Y Hu, ZW Tao, JH Tian, YY Pei, ML Yuan, YL Zhang, FH Dai, Y Liu, QM Wang, JJ Zheng, L Xu, E C Holmes and YZ Zhag. A new Corona virus associated with human respiratory disease in China. *Nature* 2020; **579**, 265-9.

[6] JF Chan, KH Kok, Z Zhu, H Chu, KK To, S Yuan and KY Yuen. Genomic characterization of the 2019 novel humanpathogenic coronavirus isolated from a patient with atypical pneumonia after visiting Wuhan. *Emerg. Microb. Infect.* 2020; **9**, 221-36.

[7] C Gil, T Ginex, I Maestro, V Nozal, L Barrado-Gil, MA Cuesta-Geijo, J Urquiza, D Ramírez, C Alonso, NE Campillo and A Martinez. COVID-19: Drug targets and potential treatments. *J. Med. Chem.* 2020; **63**; 12359-86.

[8] CK Chang, SC Lo, YS Wang and MH Hou. Recent insights into the development of therapeutics against coronavirus diseases by targeting N protein. *Drug Discov. Today* 2016; **21**, 562-72.

[9] S Kang, M Yang, Z Hong, L Zhang, Z Huang, X Chen, S He, Z Zhou, Z Zhou, Q Chen, Y Yan, C Zhang, H Shan and S Chen. Crystal structure of SARS-CoV-2 nucleocapsid protein RNA binding domain reveals potential unique drug targeting sites. *Acta Pharm. Sin. B* 2020; **10**, 1228-38.

[10] S Belouzard, JK Millet, BN Licitra and GR Whittaker. Mechanisms of coronavirus cell entry mediated by the viral spike protein. *Viruses* 2012; **4**, 1011-33.

[11] D Wrapp, N Wang, KS Corbett, JA Goldsmith, CL Hsieh, O Abiona, BS Graham and JS McLellan. Cryo-EM structure of the 2019-nCoV spike in the prefusion conformation. *Science* 2020; **367**, 1260-3.

[12] R Hilgenfeld. From SARS to MERS: Crystallographic studies on coronaviral proteases enable antiviral drug design. *FEBS J.* 2014; **281**, 4085-96.

[13] B Kolita, AJ Bora and P Hazarika. A Search of COVID-19 main protease inhibitor from plant derived alkaloids using chloroquine and hydroxychloroquine as reference: An *in-silico* approach. *Int. J. Sci. Res. Biol. Sci.* 2020; **7**, 51-61.

[14] Y Zhao, C Fang, Q Zhang, R Zhang, X Zhao, Y Duan, H Wang, Y Zhu, L Feng, J Zhao, M Shao, X Yang, L Zhang, CPeng, K Yang, D Ma, Z Rao and K Yang. Crystal structure of SARS-CoV-2 main protease in complex with protease inhibitor PF-07321332. *Protein Cell.* 2022; **13**, 689-93.

[15] KC Lehmann, EJ Snijder, CC Posthuma and AE Gorbalenya. What we know but do not understand about nidovirus helicases. *Virus Res*. 2015; **202**, 12-32.

[16] Z Jia, L Yan, Z Ren, L Wu, J Wang, JGuo, L Zheng, Z Ming, L Zhang, Z Lou and Z Rao. Delicate structural coordination of the severe acute respiratory syndrome coronavirus Nsp13 upon. *Nucleic Acids Res.* 2019; **47**, 6538-50.

[17] O Altay, E Mohammadi, S Lam, H Turkez, J Boren, J Nielsen, M Uhlen and A Mardinoglu. Current status of COVID-19 therapies and drug repositioning applications. *iScience* 2020; **23**, 101303.

[18] L Cynthia, Z Qiongqiong, L Yingzhu, LV Garner, SP Watkins, LJC Smoot, AC Gregg, AD Daniels, S Jervey and D Albaiu. Research and development on therapeutic agents and vaccines, for COVID-19 and related human coronavirus diseases. *ACS Cent. Sci.* 2020; **6**, 315-31.

[19] H Li, YM Wang, JY Xu and B Cao. Potential antiviral therapeutics for 2019 novel coronavirus. *Chin. J. Tubercul. Respir. Dis.* 2020; **43**, E002.

[20] ML Holshue, C DeBolt, S Lindquist, KH Lofy, J Wiesman, H Bruce, C Spitters, K Ericson, S Wilkerson, A Tural, G Diaz, A Cohn, LA Fox, A Patel, SI Gerber, L Kim, S Tong, X Lu, S Lindstrom, MA Pallansch, WC Weldon, …, SK Pillai. First case of 2019 novel coronavirus in the United States. *New Engl. J. Med.* 2020; **382**, 929-36.

[21] L Dong, S Hu and J Gao. Discovering drugs to treat coronavirus disease 2019 (COVID-19). *Drug Discov. Ther.* 2020; **14**, 58-60.

[22] PD Wakchaure, S Ghosh and BR Ganguly. Revealing the inhibition mechanism of RNA-dependent RNA polymerase (RdRp) of SARS-CoV-2 by remdesivir and nucleotide analogues: A molecular dynamics simulation study. *J. Phys. Chem. B* 2020; **124**, 10641-52.
[23] L Caly, DJ Druce, MJ Catton, DA Jans and KM Wagstaff. The FDA-approved drug ivermectin inhibits the replication of SARS-CoV-2 *in vitro*. *Antivir. Res.* 2020; **178**, 104787.
[24] MA Pinzon, S Ortiz, H Holguın, JF Betancur, AD Cardona, H Laniado, CA Arias, B Muñoz, J Quiceno, D Jaramillo and Z Ramirez. Dexamethasone vs methylprednisolone high dose for Covid-19 pneumonia. *PLoS One* 2021; **16**, e0252057.
[25] OT Ebob, SB Babiaka and F Ntie-Kang. Natural products as potential lead compounds for drug discovery against SARS-CoV-2. *Nat. Prod. Bioprospect.* 2021; **11**, 611-28.
[26] CY Wu, JT Jan, SH Ma, CJ Kuo, HF Juan, YS Cheng, HH Hsu, HC Huang, D Wu, A Brik, FS Liang, RS Liu, JM Fang, ST Chen, PH Liang and CH Wong. Small molecules targeting severe acute respiratory syndrome human coronavirus. *PNAS* 2004; **10**, 10012-7.
[27] CC Wen, YH Kuo, JT Jan, PH Liang, SY Wang, HG Liu, CK Lee, ST Chang, CJ Kuo, SS Lee, CC Hou, PW Hsiao, SC Chien, LF Shyur and NS Yang. Specific plant terpenoids and lignoids possess potent antiviral activities against severe acute respiratory syndrome coronavirus. *J. Med. Chem.* 2007; **50**, 4087-95.
[28] CW Lin, FJ Tsai, CH Tsai, CC Lai, L Wan, TY Ho, CC Hsieh and PDL Chao. Anti-SARS coronavirus 3C-like protease effects of Isatis indigotica root and plant-derived phenolic compounds. *Antivir. Res.* 2005; **68**, 36-42.
[29] YB Ryu, HJ Jeong, JH Kim, YM Kim, JY Park, D Kim, TTH Nguyen, SJ Park, JS Chang, KH Park, MC Rho and WS Lee. Biflavonoids from Torreya nucifera displaying SARS-CoV 3CL (pro) inhibition. *Bioorg. Med. Chem.* 2010; **18**, 7940-7.
[30] PW Cheng, LT Ng, LC Chiang and CC Lin. Antiviral effects of saikosaponins on human coronavirus 229E *in vitro*.*Clin. Exp. Pharmacol. Physiol.* 2006; **33**, 612-6.
[31] DW Kim, KH Seo, MJ Curtis-Long, KY Oh, JW Oh, JK Cho, KH Lee and KH Park. Phenolic phytochemical displaying SARS-CoV papain-like protease inhibition from the seeds of Psoralea corylifolia. *J. Enzym Inhib. Med. Chem.* 2014; **29**, 59-63.
[32] J Cinatl, B Morgenstern, G Bauer, P Chandra, H Rabenau and HW Doerr. Glycyrrhizin, an active component of liquorice roots, and replication of SARS-associated coronavirus. *Lancet* 2003; **361**, 2045-6.
[33] QY Yang, XY Tian and WS Fang. Bioactive coumarins from *Boenninghauseniasessilicarpa*. *J. Asian Nat. Prod. Res*. 2007; **9**, 59-65.
[34] SY Li, C Chen, HQ Zhang, HY Guo, H Wang, L Wang, X Zhang, SN Hua, J Yu, PG Xiao, RS Li and X Tan. Identification of natural compounds with antiviral activities against SARS-associated coronavirus. *Antiviral Res*. 2005; **67**, 18-23.
[35] JY Kim, YI Kim, SJ Park, IK Kim, YK Choi and SH Kim. Safe, high-throughput screening of natural compounds of MERS-CoV entry inhibitors using a pseudovirus expressing MERS-CoV spike protein. *Int. J. Antimicrob. Agents* 2018; **52**, 730-2.
[36] DE Kim, JS Min, MS Jang, JY Lee, YS Shin, JH Song, HR Kim, S Kim, YH Jin and S Kwon. Natural bis-benzylisoquinoline alkaloids-tetrandrine, fangchinoline, and cepharanthine, inhibit human coronavirus OC43 infection of MRC-5 human lung cells. *Biomolecules* 2019; **9**, 696.
[37] TY Ho, SL Wu, JC Chen, CC Li and CY Hsiang. Emodin blocks the SARS coronavirus spike protein and angiotensin-converting enzyme 2 interaction. *Antivir. Res.* 2007; **74**,92-101.
[38] YB Ryu, SJ Park, YM Kim, JY Lee, WD Seo, JS Chang, KH Park, MC Rho and WS Lee. SARS-CoV 3CL pro inhibitory effects of quinone-methidetriterpenes from Tripterygiumregelii. *Bioorg. Med. Chem. Lett.* 2010; **20**, 1873-6.
[39] L Chen, J Li, C Luo, H Liu, W Xu, G Chen, OW Liew, W Zhu, CM Puah, X Shen and H Jiang. Binding interaction of quercetin-3-beta-galactoside and its synthetic derivatives with SARS-CoV3CL(pro): Structure-activity relationship studies reveal salient pharmacophore features. *Bioorg. Med. Chem.* 2006; **14**, 8295-306.
[40] JY Park, JH Kim, YM Kim, HJ Jeong, DW Kim, KH Park, HJ Kwon, SJ Park, WS Lee and YB Ryu. Tanshinones as selective and slow-binding inhibitors for SARS-CoV cysteine proteases. *Bioorg. Med. Chem.* 2012; **20**, 5928-35.
[41] JY Park, HJ Jeong, JH Kim, YM Kim, SJ Park, D Kim, KH Park, WS Lee and YB Ryu. Diarylheptanoids from Alnus japonica inhibit papain-like protease of severe acute respiratory syndrome coronavirus. *Biol. Pharm. Bull.* 2012; **35**, 2036-42.

[42] MS Yu, J Lee, JM Lee, Y Kim, YW Chin, JG Jee, YS Keum, YJ Jeong. Identification of myricetin and scutellarein as novel chemical inhibitors of the SARS coronavirus helicase, nsP13. *Bioorg. Med. Chem. Lett.*2012; **22**, 4049-54.
[43] JY Park, JA Ko, DW Kim, YM Kim, HJ Kwon, HJ Jeong, CY Kim, KH Park, WS Lee and YB Ryu. Chalcones isolated from Angelica keiskei inhibit cysteine proteases of SARS-CoV. *J. Enzyme Inhib. Med. Chem.* 2016; **31**, 23-30.
[44] R Thomsen and MH Christensen. MolDock: A new technique for high-accuracy molecular docking. *J. Med. Chem.* 2006; **49**, 3315-21.
[45] DK Gehlhaar, D Bouzida and PA Rejto. Fully automated and rapic flexible docking of inhibitors covalently bound to serine proteases. *In*: Proceedings of the 7th International Conference on Evolutionary Programming, California, United States. 1998.
[46] JM Yang and CC Chen. GEMDOCK: A generic evolutionary method for molecular docking. *Proteins* 2004; **55**, 288-304.
[47] F Cheng, W Li, Y Zhou, J Shen, Z Wu, G Liu, PW Lee and Y Tang. admetSAR: A comprehensive source and free tool for assessment of chemical ADMET properties. *J. Chem. Inform. Model.* 2012; **52**, 3099-105.
[48] CA Lipinski, F Lombardo, BW Dominy and PJ Feeney. Experimental and computational approaches to estimate solubility and permeability in drug discovery and development settings. *Adv. Drug Deliv. Rev.* 1997; **46**, 3-26.
[49] GA Jeffrey. *An introduction to hydrogen bonding*. Oxford University Press, Oxford, United Kingdom, 1992.
[50] JA Williams, R Hyland, BC Jones, DA Smith, S Hurst, TC Goosen, V Peterkin, JR Koup and SE Ball. Drug-drug interactions for UDP-glucuronosyltransferase substrates: A pharmacokinetic explanation for typically observed low exposure (AUCi/AUC) ratios. *Drug Metab. Dispos.* 2004; **32**, 1201-8.
[51] M Kacevska, GR Robertson, SJ Clarke and C Liddle. Inflammation and CYP3A4-mediated drug metabolism in advanced cancer: Impact and implications for chemotherapeutic drug dosing. *Expet. Opin. Drug Metab. Toxicol*. 2008; **4**, 137-49.
[52] KE Lasser, PD Allen, SJ Woolhandler and DU Himmelstein, SM Wolfe and DH Bor. Timing of new black box warnings and withdrawals for prescription medications. *JAMA* 2002; **287**, 2215-20.
[53] LC Wienkers, TG Heath. Predicting *in vivo* drug interactions from *in vitro* drug discovery data. *Nat Rev. Drug Discov*. 2005; **4**, 825-33.